Original Research Article

AERO-MAGNETIC AND AERO-RADIOMETRIC PROSPECTING FOR POTENTIAL GOLD MINERALISATION ~~POTENTIALS~~ OVER ILESHA AND ITS ENVIRONS, SOUTHWEST NIGERIA

ABSTRACT

The mapping of potential gold mineralization zones ~~potential zones~~ in a part of southwestern Nigeria was carried out from the analyses and interpretation of airborne magnetic and radiometric data. Some enhancing filters, such as analytic signal, first vertical derivative ~~was~~ were applied on the Total Magnetic Intensity map to delineate near-surface structures that might host the potential mineral zones ~~potential~~ within the study area. The analytic signal shows three magnetic zones delineated with low magnetic zone ranging from 0.008 to 0.026 nT/m, moderate with amplitude 0.117 to 0.029 nT/m and high with amplitudes above 0.109 nT/m. In the First vertical derivative, NE-SW structural trends, considered to be the orientation~~s~~ of gold mineral deposits dominate~~s~~. The depth obtained from the source parameter imaging ranges from 89.03 to 574.76 m. The results from the analysis of aero-radiometric data revealed that the concentration of the radioelements ranged from 0.16 – 3.25 %, 0.80 – 33.27 ppm and 0.13 – 7.24 ppm for potassium, thorium, and uranium, respectively. The K/eTh ratio maps reveal the presence of hydrothermal alteration zones at the north-eastern, central, and southern parts of the study area corresponding to the amphibolite schist and quartz schist, respectively, ~~a~~ source rocks for gold deposits. This study has shown that the structures (faults and fractures) and hydrothermal alteration zones delineated within the study area are favourable features to host gold mineralization in the study area.

Keywords: Aero-magnetic, Aero-radiometric, Analytic signal, Hydrothermal alteration, Au-Mineralization, Nigeria.

1. Introduction

Nigeria's economy like other oil-dependent economy of a few countries was severely affected by the global shock witnessed in the second half of 2014 and the present 2020 global economic meltdown resulted from the Covid-19 pandemic that almost all the economic indices were negatively affected and growth plummeted. The country is in a downward spiral of economic damages like other oil-dependent countries, due to the plunge in the world oil prices (Fayemi, 2017). In order to achieve the goal of the present study, namely the search for the potential gold deposits is equivalent to the search for the subsurface geologic features, such as~~;~~ faults, folds, fractures, veins, and shear zones, and hydrothermally altered zones that are favourable features for gold mineralisation (Junner, 1940).

According to Ajeigbe *et al.*, (2014), geologic structures (faults, folds, fractures, veins, and shear zones, and hydrothermally altered zones and lithology) have a very important role in the emplacement of mineralization.

Under certain circumstances which occur fairly commonly, structural conditions are reflected significantly in the trends and intensities apparent on aeromagnetic maps.

Mineralisation processes affect the concentration of radioelements in rocks, and, hence, radiometric method~~,~~ ~~therefore~~ becomes a useful tool in identification of potential mineralized zones (Ogungbemi, 2018). Radiometric surveys are capable of directly detecting the presence of Uranium, Thorium and Potassium which also assist~~s~~ in locating some intrusive-related mineral deposits. Therefore, the integration of the airborne magnetic and radiometric dataset will aid in the mineralisation-mapping. ~~In particular,~~ The measurement of earth's magnetic field intensity is referred to as magnetic method which involves the measurement of horizontal or vertical components (Mekonnen, 2004). In spite of the fact that gold deposits are non-magnetic, the magnetic method is used because gold is closely related to pyrite which is also non-magnetic. Since pyrite is metamorphosed into pyrrhotite at the upper greenschist-lower amphibolite grades and also pyrrhotite is metamorphosed into magnetite (Keary *et al.*, 2002 and Christopher 2013), as such, minerals that comprise~~s of~~ pyrrhotite and magnetite are easily delineated using the airborne magnetic survey.

2. Location and Geology of the ~~s~~Study A~~a~~rea

The study area (Figure 1) is bounded by geographic latitudes 7°00′N and 8°00′N and geographic longitude 4°00′E and 5°00′E within the Precambrian of southwestern Nigeria. It covers a total land area of approximately 12100 km^2. The average rainfall of the area ranges from 1125 mm in derived savannah to 1475 mm in the rain-forest belt. The mean annual temperature ranges from 27.2°C in the month of June to 39.0°C in December. The basement rocks of Nigeria are part of the extensive Pan-African Province of West Africa and are delimited in the west by the West African Craton and east by the Congo Craton. Nigeria basement comprises the Migmatite-gneiss complex, the Schist-belts and the Older Granites. The Migmatite Gneiss Complex is the oldest, most widespread and abundant rock type in the basement. It is of the Archean-Proterozoic age and a product of long, protracted and, possibly, polycyclic evolutionary histories. The Nigerian Schist-belts comprise ~~of~~ low-grade metasediments and metamorphosed pelitic and psammitic assemblages that outcrop in a series of N-S trending synformal troughs unfolded into the crystalline complex of migmatite-gneiss. The Older Granite which is also known as Pan-African Granites include rocks of wide range of composition varying from tonalite, granodiorite, granite and syenite (Rahaman, 1976). The Ijero-pegmatite form an intrusion into the biotite-schist that occupies the central part of the study area. The study area is an extension of the eastern end of Ife-Il~~j~~esha Schist-belt and falls within the Basement Complex of southwestern Nigeria.

The major rock associated with the Ilesha and other part of the study area forms a part of the Proterozoic schist belts of Nigeria (Figure 2), which are predominantly, developed in the western half of the country. In terms of structural features, lithology and mineralization, the schist belts of Nigeria show considerable similarities to the Archaean Green Stone Belts. Rocks in Ilesha and other parts of this study area are structurally divided into two main segments by two major fracture zones often called the Iwaraja faults in the eastern part and the Ifewara faults in the western part. ~~The major rocks associated with the area form part of the Proterozoic schist belts in Nigeria as shown in Figure 2.~~ Migmatite – Gneiss ~~c~~Complex,~~;~~ Quartz – Schist,~~;~~ Quartzite,~~;~~ Amphibolites,~~;~~ Granite – Gneiss,~~;~~ Amphibolites schist and porphyritic granite are the major rocks in the area, as delineated in Figure 2. Other minor rocks, according to ~~(~~Rahaman~~,~~ (1976), are Garnet, Quartz Chlorite bodies and Dol~~e~~~~o~~rites.

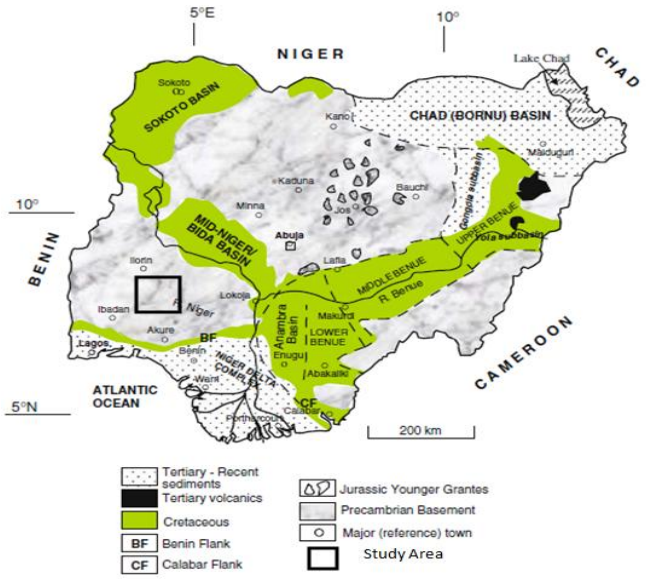

Figure 1: Geological Map of Nigeria showing the study area in black outline (Source: Obaje, 2009).

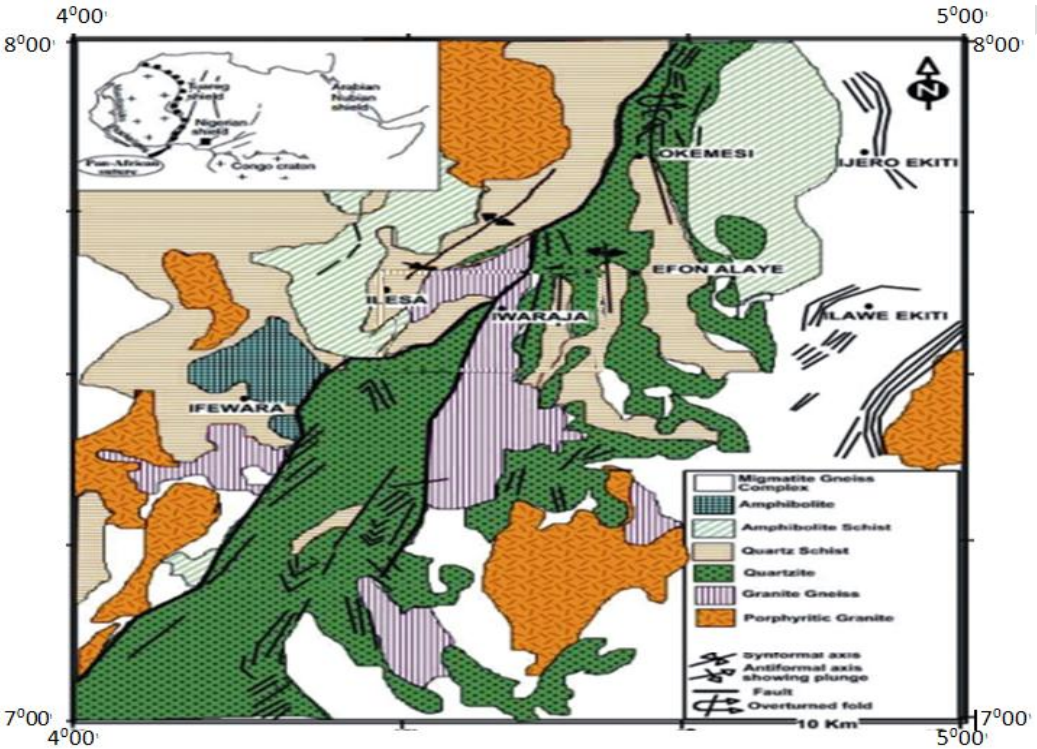

Figure 2: Geological map of the study area over Ilesha and its environs~~ment~~

3. Materials and Method

Aero-magnetic and aeroradiometric data procured from the Nigerian Geological Survey Agency (NGSA) is part of the data obtained during the high-resolution airborne geophysical survey of Nigeria, involving magnetic, radiometric, and limited electromagnetic survey in 2009 by Fugro Airborne survey. The aero-magnetic data ~~was~~ were obtained using a proton magnetometer with resolution of 0.01 nT. The data were

acquired at flight height of 80 m emphasizing high resolution survey, with line-spacing of 500 m and tie line spacing of 5,000 m. The four aero-magnetic and aeroradiometric data sheets are 242 (Iwo), 243 (Ilesha), 262 (Apomu) and 263 (Ondo), which correspond to latitude 7^0N to 8^0N and longitude 4^0E to 5^0E. Each scaled 1:100,000 topographical sheet covers an area of about 3025 km^2 (55 km x 55 km) totalling a superficial area of 12,100 km^2. The digitized data were filtered using a low pass Fourier domain sub-routine filter to eliminate unwanted wavelengths and to pass longer wavelengths.

3.1 Data Processing and Enhancement

3.2 Regional and residual separation

The interpretation of the magnetic field begins with the separation of the long-wavelength anomalies of the regional field component, which is attributed to deep and large scale sources from the shorter wavelength features constituting the residual field assumed to arise from shallow and small scale sources. The residual data is obtained as a derivative of the total field data.

Total Field = Regional Field - Residual Field -/+ ? (1)

Residual Field = Total Field - Regional Field (2)

3.3 Analytic signal

The application of analytic signals to magnetic interpretation was pioneered by (Nabighian, (1972), for 2D case, primarily as an apparatus for computing depth and position of sources to be used to complement objective one and three results obtained with Euler deconvolution. The analytic signal method which is also known as total gradient method is a notable method for establishing the edges of magnetic anomalies. It is formed through the combination of the horizontal and vertical gradients of the magnetic anomaly. The analytic signal is not dependent of magnetization direction and Earth's magnetic field direction. This implies that all bodies with similar geometry have the same analytical signal (Milligan and Gunn, 1997).

It is based on the calculation of the first derivatives of magnetic anomalies to estimate source characteristics. The function used in the analytic signal technique is the analytic signal amplitude (absolute value) of the observed magnetic field at the location (x, y), described by three orthogonal gradients of the total magnetic field via the expression:

$$|A(x,y)| = \sqrt{(\frac{\partial \mathrm{M}}{\partial \mathrm{x}})^2 + (\frac{\partial \mathrm{M}}{\partial \mathrm{y}})^2 + (\frac{\partial \mathrm{M}}{\partial \mathrm{z}})^2} \quad (3)$$

where:; A (x, y) = amplitude of the analytic signal at (x, y),

M = observed magnetic field at (x, y).

3.4 First vertical derivatives

The first vertical derivative or vertical gradient can be thought of as component of the rate of change of the anomaly values as the potential field data are upward continued. First vertical derivative can be applied either in space or frequency domain. It is proposed by (Nabighian, (1984), using 3D Hilbert transforms in the x and y directions. It is used to enhance shallow features with their boundaries and associated lineaments. It amplifies short-wavelengths at the expense of longer anomalies related to deep sources.
It is formulated thus:

$$VDR = \frac{\partial \mathrm{M}}{\partial \mathrm{z}} \quad (4)$$

The vertical gradient helps resolve closely-spaced short-wavelength anomalies (Reeves, 2005). This filter is useful to emphasize shallow structures such as networks of faults, fractures and dykes as stated in objective one and two.

3.5 Source Parameter Imaging (SPI^{TM})

The Source Parameter Imaging (SPI^{TM}) is a technique using an extension of the complex analytical signal to evaluate magnetic depths. The SPI^{TM} function is a fast, simple, and powerful method for calculating the depth of magnetic sources. Its accuracy has been shown to be +/- 20% in tests on real data sets with drill-hole control. This accuracy is analogous to that of Euler deconvolution; however, SPI has the advantage of producing a more complete set of coherent solution points and it is easier to use (Salako, 2014). One merit of the SPI technique is that the depth can be visualized in a raster format and the true thickness determined for each anomaly.

The SPI method (Thurston and Smith, 1997) estimates the depth parameter using the local wave number of the analytical signal. The analytical signal $A_1(x, z)$ is defined by Nabighian (1972) as:

$$A_1(x,z) = \frac{\partial \mathrm{M(x,z)}}{\partial \mathrm{x}} - \mathrm{j}\frac{\partial \mathrm{M(x,z)}}{\partial \mathrm{z}} \quad (5)$$

~~W~~where:

$A_1(x,z)$ = Analytic signal $\Leftrightarrow$

M (x, z) = magnitude of the anomalous total magnetic field,

j = imaginary number, z and x indicate the gradients in the vertical and horizontal direction. Also, it was shown by Nabighian (1972) that the gradient changes constitute the real and imaginary parts of the 2D analytical signal are related as follows:

$$\frac{\partial \mathrm{M(x,z)}}{\partial \mathrm{x}} \Leftrightarrow -\mathrm{j}\frac{\partial \mathrm{M(x,z)}}{\partial \mathrm{z}} \quad (6)$$

where:~~;~~$\Leftrightarrow$ implies a Hilbert transform.
Thurston and Smith (1972) defined the local wave number K_1 to be:

$$k_1 = \frac{\partial}{\partial \mathrm{x}}\tan^{-1}\left[\frac{\partial \mathrm{M}}{\partial \mathrm{z}} \Big/ \frac{\partial \mathrm{M}}{\partial \mathrm{x}}\right] \quad (7)$$

The Hilbert transform and the vertical derivative operators are linear, so the vertical derivative of (2.0) will give the Hilbert transform pair,

$$\frac{\partial^2 \mathrm{M(x,z)}}{\partial \mathrm{z}\,\partial \mathrm{x}} \Leftrightarrow -\frac{\partial^2 \mathrm{M(x,z)}}{\partial^2 \mathrm{z}} \quad (8)$$

Thus, the analytic signal could be defined based on second-order derivatives, $A_2(x,z)$, where:~~;~~

$$A_2(x,z) = \frac{\partial^2 \mathrm{M(x,z)}}{\partial \mathrm{z}\,\partial \mathrm{x}} - \mathrm{j}\frac{\partial^2 \mathrm{M(x,z)}}{\partial^2 \mathrm{z}} \quad (9)$$

This gives rise to a second order local wave number κ_2, where:

$$k_2 = \frac{\partial}{\partial \mathrm{x}}\tan^{-1}\left[\frac{\partial^2 \mathrm{M}}{\partial^2 \mathrm{z}} \Big/ \frac{\partial^2 \mathrm{M}}{\partial \mathrm{z}\,\partial \mathrm{x}}\right] \quad (10)$$

This first- and second-order local wave numbers are used to determine the most appropriate model and depth estimate of any assumption about a model.

The analytic signal amplitude maximizes over the edge of the magnetic structures. aAs a result, the high magnetic anomalies zones are associated with highly rich ferromagnesian-bearing rocks with minor felsic minerals (Telford 1990). Tawey *et al*. (2020), emphasized that the analytic signal is used in locating contacts and sheet-like structures by forming maxima around the edges of magnetic sources.

3.6 Airborne Radiometric Survey method

Geophysical radiometric survey also known as Gamma-Ray Spectrometry is a passive geophysical technique that is utilized to examine the subsurface of the Earth and it deals with the estimation of the spatial distribution of three radioactive elements (potassium-K, thorium-Th and uranium-U) in the top 30 - 40 cm of the earth's crust by detecting and estimating the intensities of the gamma rays produced by these elements in a radioactive decay (IAEA, 2003). The Airborne Radiometric Survey method is efficient in lithological discrimination and can reproduce geological contacts with high accuracy (depending on the spacing of the measurements) because the mapped information is provided by radiation that emanates only from a very shallow depth. In the present study, the method enables the location of geological boundaries and compositional zoning within geological units.

3.7 Natural radioactivity of rocks

The Uranium and Thorium in igneous rocks are concentrated much in a few accessory minerals such as zircon, sphene and apiatite (Slagstad, 2008). Other notable radioactive minerals, such as pyrochlore, thorite, monazite, uraninite, and allanite, are prevalent in nature but are negligible constituents of rocks, and are spread unevenly. The minerals that transmit thorium and uranium are commonly associated with felsic intrusions - specifically with younger intrusions; they can be found substantially less in mafic rocks. or in volcanic. The Uranium and Thorium content of rocks usually increases with acidity, with the maximum concentrations located in pegmatites, (Slagstad, 2008). The highest concentrations of uranium and thorium in sedimentary rocks are generally found in shales.

For Potassium, it is predominantly concentrated in feldspars and micas; rocks with none of these minerals have very low potassium. Therefore, mafic and ultramafic rocks have very low potassium content. The potassium substance of sedimentary rocks is highly variable; however, it tends to be higher in shale than in carbonates or sandstones.

3.8 Gridded Channels of K, U, Th, Ratio Maps and Ternary Map

Production of Ratio and ternary image helps in the identification and mapping of zones that are hydrothermally altered. A decrease in Th and an increase in K is indicative of alteration environment in an ore deposit (Ostrovskiy, 1975). A low Uuranium concentration with a high potassium concentration would lead to a low values of U/K ratio which is indicative of granitoid rocks. The depletion of Uuranium leaves negative aureoles which is the results of pervasive hydrothermal alteration (Boyle, 1979). Even though, Tthorium is generally immobile, an enrichment of Tthorium and Ppotassium is indicative of hydrothermal alteration in some gold deposits (Silva *et al*., 2003). A composite image (Ternary) to be created using Oasis-montaj™ software in which Potassium, Thorium and Uranium are represented in red, green, and blue colours, respectively. Spatial

distribution of the radiometric intensity generated from the Ternary images is to be compared or correlated with the geological structures and lithology of the area.

4. Results and Discussion

The airborne magnetic method is based on the measurement of the ambient magnetic susceptibility of geologic bodies and the use of the acquired data to determine the distribution of magnetic minerals (changes in lithology). Radiometric method in exploration is a measure of variations in the radio-elemental mineral (potassium, thorium and uranium) composition and is directly used to map out lateral lithological changes. Integration of the data from these survey methods ~~to be~~ is used extensively for the delineation of geologic structures and metalliferous deposits within ~~the~~ a study area.

4.1 Interpretation of the Magnetic Data

4.1.1 Total magnetic Intensity

The Total Magnetic Intensity (TMI) map (Figure 3)~~,~~ reveals magnetic susceptibility ranges from -75 nT around Ifewara, Efon Alaye and Ife south to 138 nT at Ijebu East and Iragbiji. The area is characterized by major and minor magnetic anomalies trending NE-SW direction. The high magnetic signatures of about 113 nT observed as closures at Ijebu East is as a result of metasediments (kaolin,~~.~~ clay, glass sand and silica sand) obtainable in the area. A high signature of about 123 nT is observed at Obokun which indicates metasediments such as kaolin, clay, sand, and gravel underl~~a~~ained by metamorphic rocks, mainly Quartz-schist and Amphibolite which have been subjected to intense faulting. Th~~i~~ese faults~~-~~lines serve as host to gold deposits which is one of the minerals that is obtainable in the area.

The low magnetic signature ranging from -19nT to - 75nT is observed mainly around the south-eastern part of the study area around Ife south, Ifewara and Akakunmosa East area. This low is also observed in Okoro, Atiba Local government area of Oyo state at the North western corner of the area which is underlain by migmatite Gneiss complex. The Idanre hills also intrude into the study area at the south eastern region which is responsible for the low magnetic signature obtainable in the region. Sets of lineament trending NE-SW direction ~~is~~ are predominant in the area.

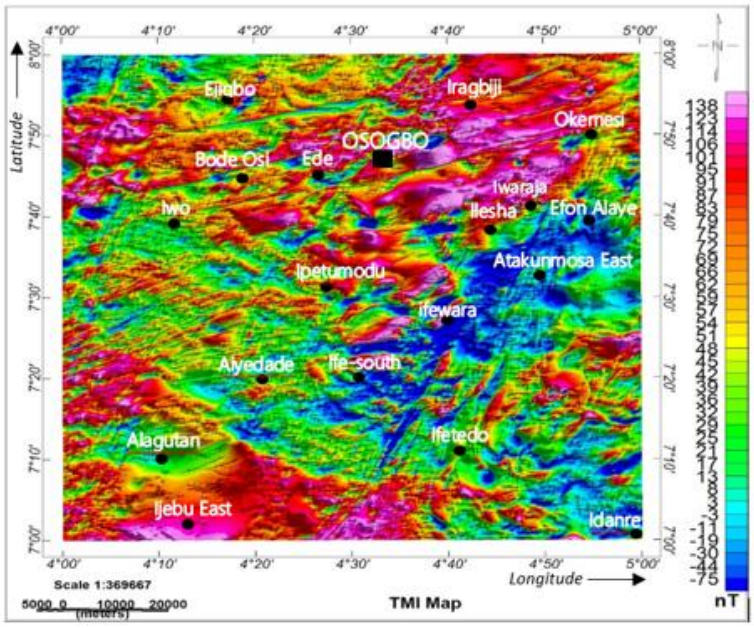

Figure 3: Total Magnetic Intensity Map of the study area (33000nT was removed)

4.1.2 Reduce to pole (RTP)

According to Tawey *et al*, 2020, to correct the effect of latitude, to realign the anomalies and have their peaks symmetrically centered over their corresponding sources because of closeness of the study area to the equator, the RTP was necessary. This helps to adjust the dependence of the data on the angle of delineation. This filtering method helps in correcting the susceptibility of the geological structures within the study area and to get the actual position of the magnetic anomalies without losing any geophysical meaning

Removal of dependence of the data on the angle of delineation, a striking difference was noted as regard the reverse in magnetic intensity between the RTP map and TMI map. However, both maps show similarities with regard the displayed anomaly in terms of the strike, width, extension and symmetry of the anomalies. Reeves C. 2005 and Tawey *et al*, 2020 pointed out that portions on the maps (Figure 4a and 4b) having alternating occurrence of magnetic high and lows could be attributed to faults/highly fractured nature of the area as oxidation in fractured zones during weathering processes commonly leads to the destruction of magnetite and as such the zones are picked out on anomaly maps as narrow zones with obviously less magnetic variation than in the surrounding rocks. The magnetic signature ranges from -129.2 nT to 71.1 nT at the RTP map.

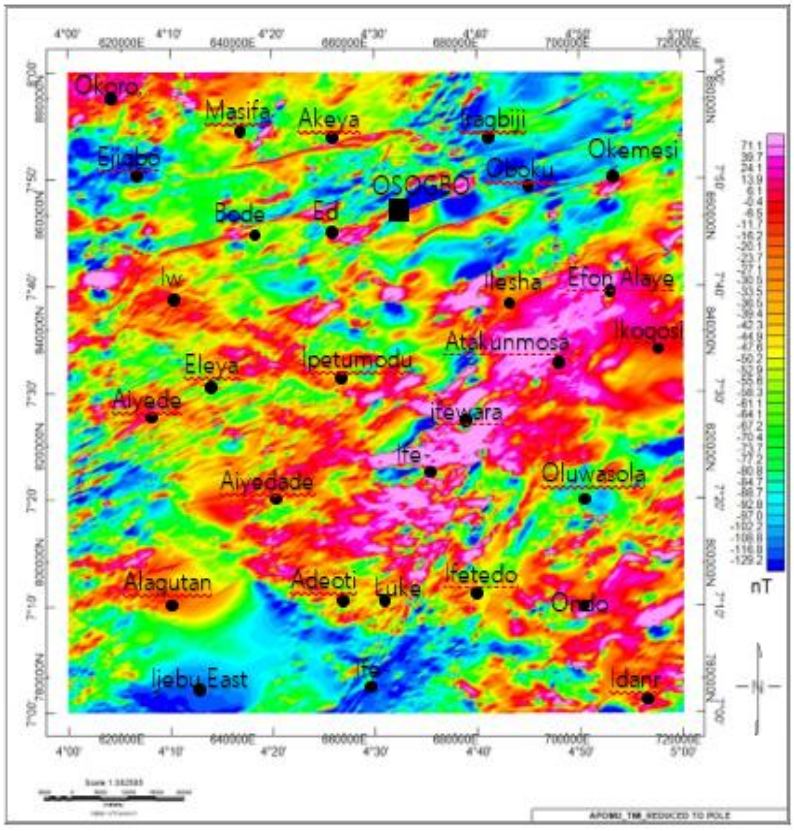

Figure 4: Reduce to Pole Map

4.1.3 First Vertical Derivative (FVD)

The FVD shown in colour shaded (Figure 5a) and grey scale (Figure 5b) enhanced the structure and lithology of the subsurface beneath the study area not observed in the TMI and RTP map. The FVD map (Figure 5a) reveals areas of high frequency (HF) and low frequency (LF).

Low frequency regions noticeable at Ijebu East area are regions overlayed by thick metasediments. Fault lines and lineaments are observed at regions of high frequencies which could be host for minerals. A major fault line in purple colour on the grey scale map (Figure 5b) cuts across the study area from the south and runs in north-east direction through Ife north, Ife south, Ifewara, Ilesha east in Osun state. This fault line also cuts through Iwaraja town which is about 2 km North of Ilesha unto Abosa ila, North east of the study area. In Figure 5b, are sets of short and long lineaments trending NE - SW directions (in cyan colour). The set of short lineament~~s~~ features observed at western edge, North, and central regions of the study area are located within the lithological boundaries of magnetic source bodies of Quartz-schist, and Granite Gneiss and cuts across Aiyede and Osegede towns in Oyo state and Eleya Aboba in Osun state. Northwards, the long lineaments are observed in towns like Ogbagba, Ibokun, Abeere, and Akeyan areas in Osun state which represent lithological boundaries and could also be interpreted as fractures or fault lines.

The high frequency magnetic anomalies in almost the entire study area~~,~~ reveals shallow depth to causative sources. Obokun, Ikogosi and Ijebu East are some of the towns with deeper depth to causative sources as a result of the presence of thick sedimentary cover.

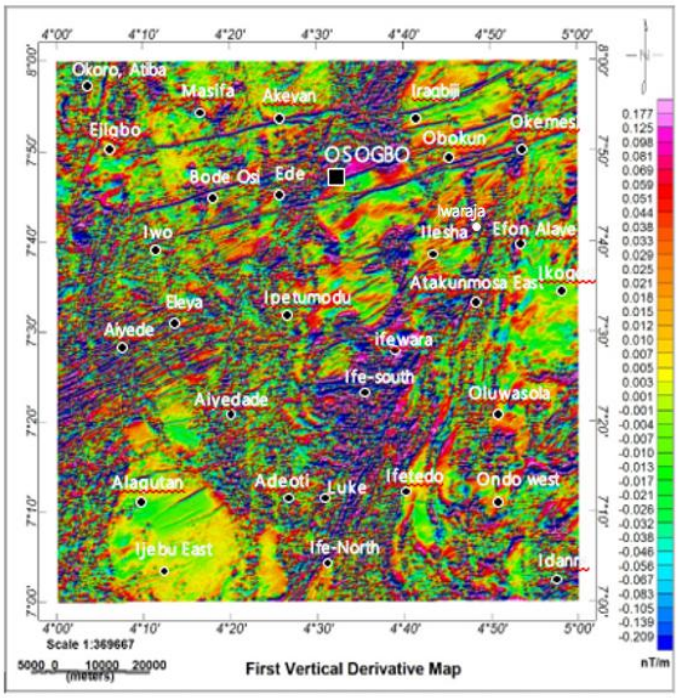

Figure 5a: First Vertical Derivative (FVD)

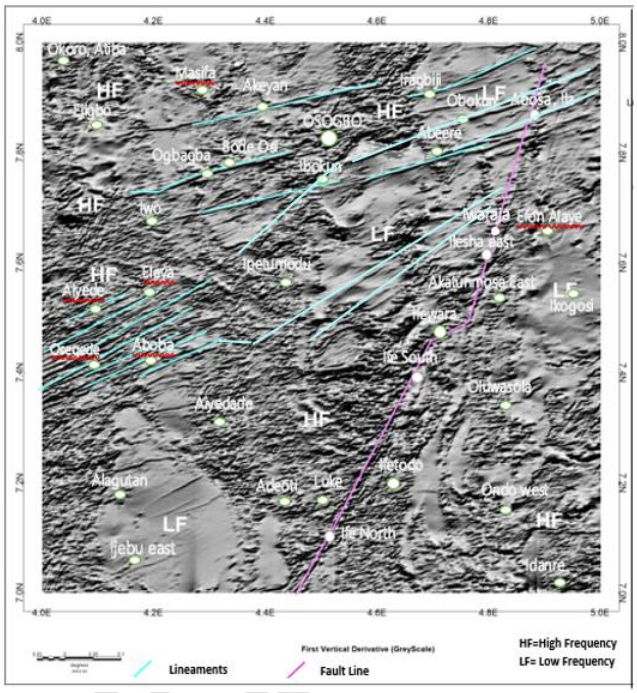

Figure 5b: First Vertical Derivative on Grey Scale

4.1.4 Analytic Signal (AS)

The amplitude of the analytical signal ranges from 0.008T/m to 0.353nT/m. From the analytic signal map (Figure 6a), structures are observed around ~~the N~~north-east and south-east of the area, and ~~also~~ span towards the western-end of the map. The AS map shows clearly the major anomalies trending mainly in the NE-SW direction as observed on the Residual Magnetic Intensity (RMI) map.

Three major zones can be ~~said to be~~ observed in this area. ~~The Low mMagnetic zone (LM) and the hHigh mMagnetic zone (HM).~~ The low magnetic (LM) zones are associated with highly weathered rocks covered by thick sediments and metasediments such as kaolin, ~~C~~clay and silica sand containing minerals such as muscovite, quartz, feldspar and anatase, and has amplitude ranging from 0.008 nT/m to 0.026nT/m. Ijebu east, Iragbiji in Ogun State and Ikogosi in Ekiti state are some of the areas in this zone. Areas associated with recent volcanic activities makes up the high magnetic (HM) zone. In this zone, magma intruded and solidified in the faults and fractures of pre-existing rocks. Ifewara, Ife north, Ife south and Osogbo, the state capital of Osun State, are some of the towns in the high magnetic zone ~~(HM)~~. The HM zone has amplitude ranging from 0.190 nT/m - 0.353nT/m. Intermediate between the LM and the HM is the moderate zone which covers about 50% of the map ranging from 0.029nT/m to 0.168nT/m with Alagutan as one of the areas in this zone.

4.1.5 Source Parameter Imaging (SPI)

The distribution of depth to causative bodies of magnetic anomalies across the study area (Figure 6b) ranges from 89.038 m to 574.763 m. The shallowest depth occurrence was recorded majorly around Aiyede, Eleya, Osogbo and Ife North which are found at the Western edge, North and Southern regions. These regions which are occupied by shallow intrusive magnetic bodies also correspond~~s~~ to regions delineated to host major

magnetic lineaments trending NE-SW direction of the study area. The South-west, South-east and North-eastern regions recorded intercalation of shallow and deep depths ranges.

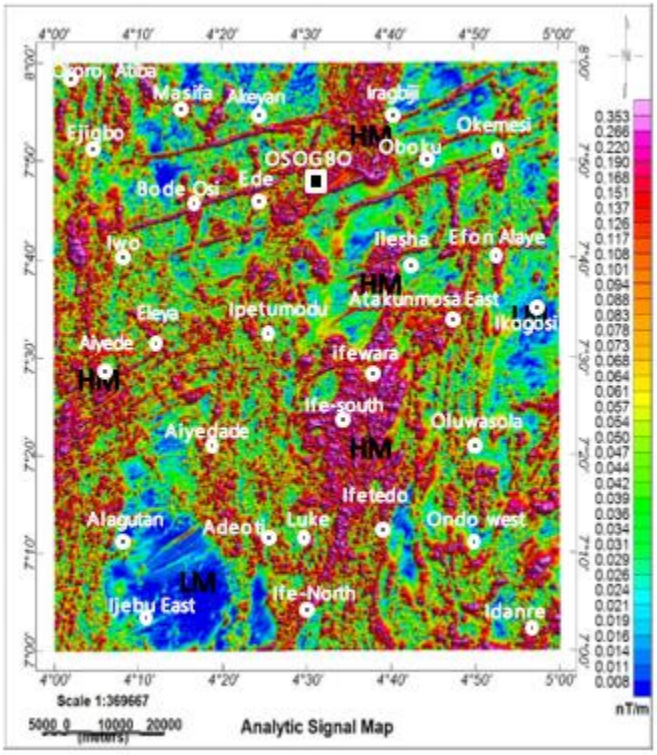

Figure 6a: Analytical signal (AS) Map

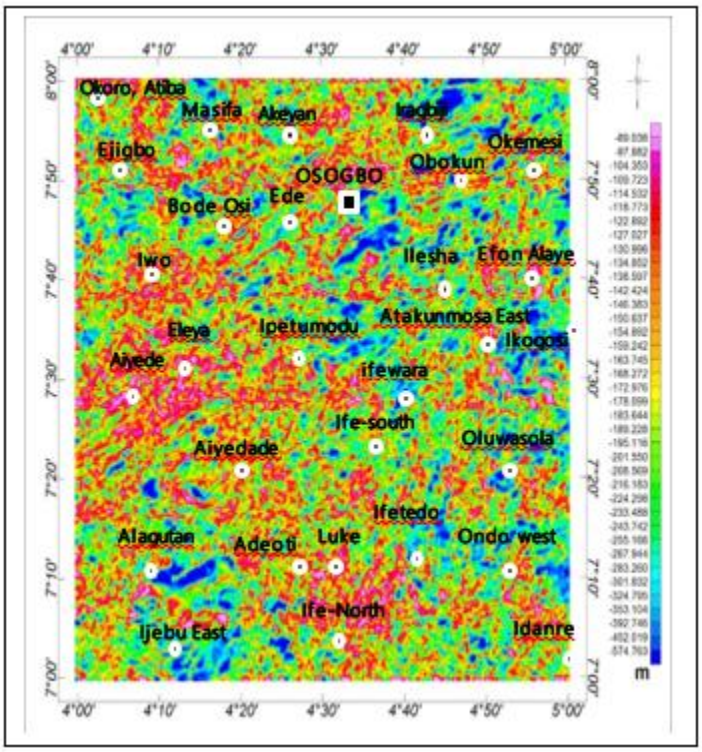

Figure 6b: Source Parameter Imaging Map

4.2 RADIOMETRIC DATA INTERPRETATIONS

4.2.1 Potassium (%K) map

The Potassium concentration (%P) map of the study area (Figure 7a) gives the Potassium concentration ranging from 0.16% to 3.25%. As alteration, weathering, climatic conditions, and hydrothermal processes has~~s~~ve effect on the concentration of radioelements (Mam *et al*. 2021 and Nicolet *et al*. 2003), potassium increases during signatures of alteration (Wilford *et al* 1997 and Mam *et al*. 2021) as a result of K-enrichment rocks present within the study area but decrease in intensity as a result of weathering (Dickson *et al*, 1997) because of its mobility. The high concentration region (colour pink) ranging from 2.08% to 3.25% are underl~~a~~ained by quartzite~~,~~ and a~~A~~mphibolite of the study area, as shown on the geology map (Figure 2). While low regions, ranging 0.16% - 0.33% with the blue coloration, are as a result of low contents of potassium and are observed to occur in small bit all over the map including the Ifewara region.

4.2.2 Thorium (Th) map

Unlike Potassium, Thorium is immobile in mineralization process but can be partly depleted in areas of intense K-alteration and silicification (Mam *et al*. 2021); hence it is not affected by alteration processes. The thorium map (Figure 7b) has thorium concentration ranging from 0.80 ppm to 33.27 ppm. High Thorium concentrations are closely related to felsic minerals and low Thorium concentrations are related to mafic minerals. The granitoids at the western and central parts of the area registered moderate to low Th concentration while those at the eastern corner registered high Th content. Thus, the regions with low thorium concentration suggest that

Th was mobilized in hydrothermally altered systems. The low Th patterns shows alteration patterns in the different rocks and along lithologic boundaries and within these zones are faults and shears which host hydrothermal fluid which leach Th concentration.

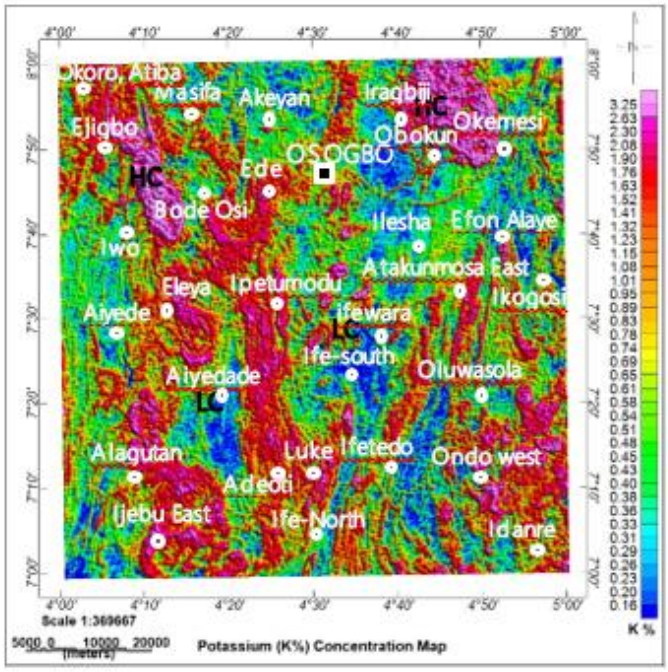

Figure 7a: Potassium concentration map (K %)

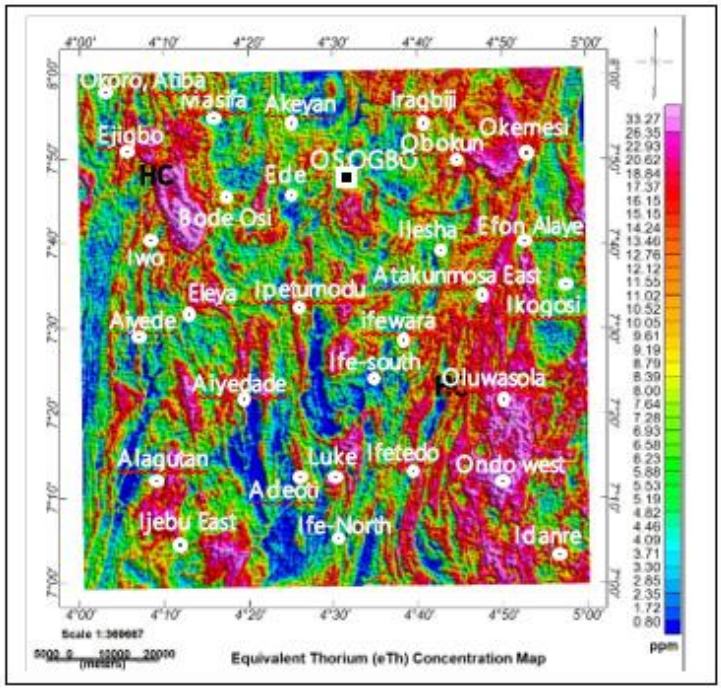

Figure 7b: Thorium concentration map

4.2.3 Uranium (eU) map

The Uranium concentration map (Figure 7c) shows Uranium concentration ranging from 0.13 ppm to 7.24 ppm. Like potassium, uranium is a very mobile element ~~according to Mam *et al*. (2021)~~ in hydrothermal and other geological processes (Mam *et al*., 2021) and an enrichment of uranium may or may not be accompanied by an enrichment of potassium (Airo, 2007). From the eU map, eU concentration can be group into high (>3.91 ppm), moderate (1.48 ppm – 3.91 ppm) and the low concentration (<1.48 ppm). Okemesi, Oluwasola and Ondo west are some of the areas underlaid by high uranium concentration. At Aiyede and Aiyedade at the west of the study area is observed low eU concentration. Moderate concentration of eU is seen around Ipetumodu, Adeoti and Luke areas.

4.2.4 Potassium Thorium Ratio Maps (K/Th)

The Potassium - Thorium (K/Th) concentration map ~~in~~ (Figure 8) depicts some lithology contacts and enhances alterations signatures. High K and low concentration of Th are associated with alterations in many ore deposits (Ostrovskiy, 1975). These occur as a result of the K-enrichment rocks which are not accompanied by the Th during hydrothermal alteration process (Dickson and Scott, 1997). This assertion makes the K/Th ratio map important when searching for signatures associated with hydrothermal alteration zones. The increase in potassium content in K/Th ratio map accompanied by Quartzite region is indicative of hydrothermal alterations.

Peak values of K/Th in pink are observed in Ede town southwards through to Adeoti within the study area and at Aiyede and Eleya, west of the study area. This is clear indication of K-enrichment due to alteration and, thus, potent host for gold mineralization. These regions when compared with the geology map (Figure 2) are occupied by ~~A~~amphibolites schist, ~~Q~~quartz schist and quartizites, ~~rocks~~ which may be potential hosts for gold.

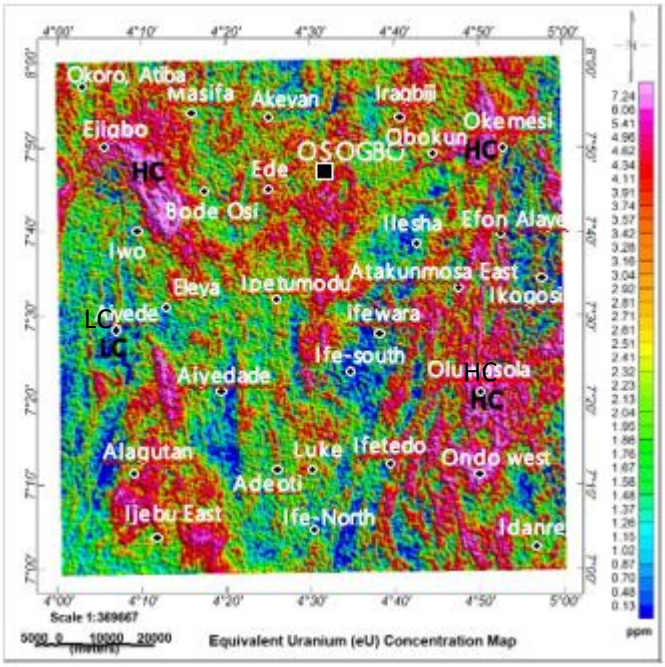

Figure 7c: Uranium concentration (eU) map

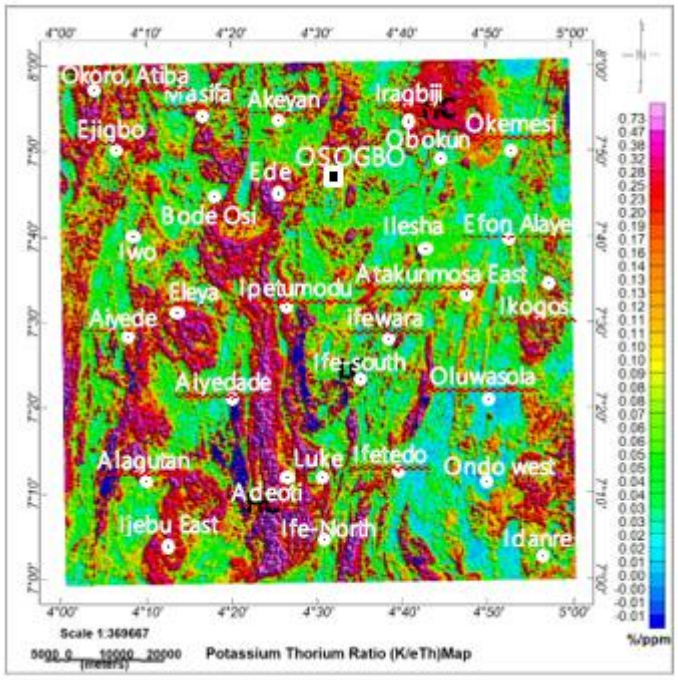

Figure 8: Potassium and Thorium Ratio (K/Th) map

4.2.5 Ternary Map

Different rock types display different concentration characteristics of the three main radioactive elements (K, Th and eU). The RGB Ternary map (Figure 9) of the study area shows the variations of the three radioelements with red, green, and blue colours representing high concentration of Potassium, Thorium and Uranium, respectively, in the regions observed. Colours other than the three primary colours are indicative of regions of well-defined proportion of two or all three of the radioelements. Parts with relatively high concentrations of all radioelements (High K, Th, and eU} appear as white and are promising regions for exploration of minerals. Regions with relatively low concentration (Low K, eTh, and eU} appear as black to brown colours. Cyan colour zones indicate~~s~~ regions with high Th and eU but less K. Magenta zones are zones of high K and eU but less Th. In yellow colour are regions of high K and Th but less eU.

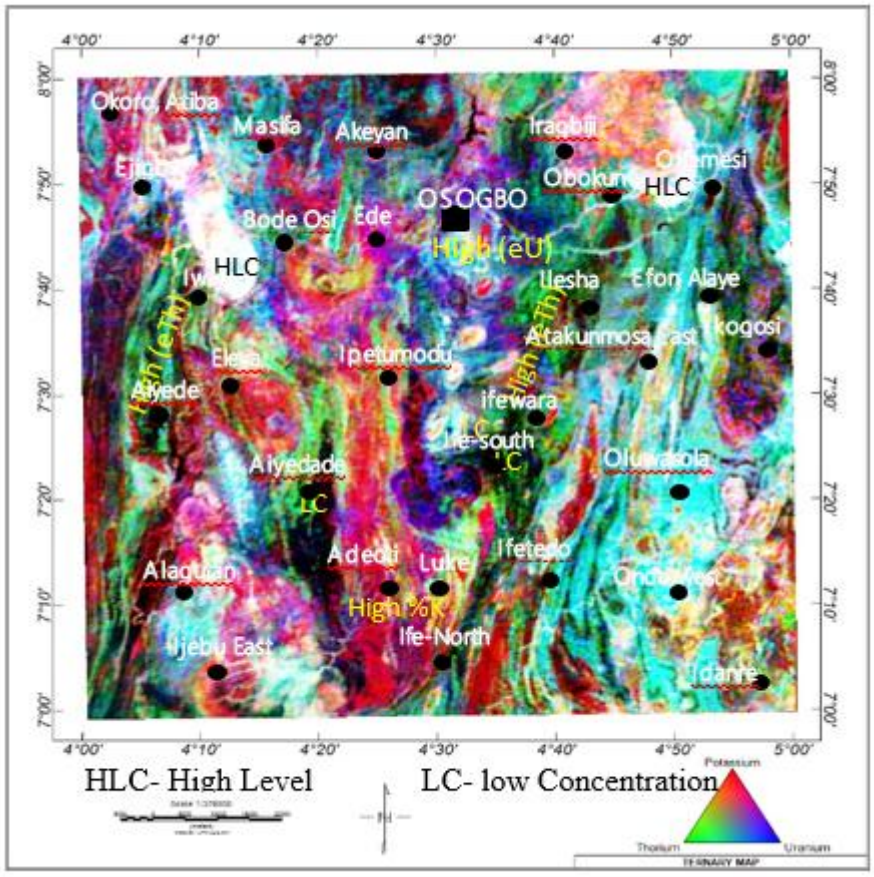

Figure 9: Ternary Map (RGB=K, eTh, eU) of the Study ~~a~~Area

5. CONCLUSION

The analysis of ~~A~~aero-radiometric and ~~A~~aero-magnetic data for gold mineralisation over Ilesha and its environs, south-western Nigeria was achieved by delineating mineralisation-potential zones through mapping lithology, structural elements, and hydrothermal alteration. The structural features are trending in the NE-SW direction and can be associated with the orientation of the mineral deposits. The direction of major lineaments also corresponds to the direction of the Ifewara and Iwaraja fault lines that run through the south-western basement complex. Ratios of the radioelements (K/Th) was analysed to verify the enrichment or depletion of radioisotopes in the area. Zones hydrothermally affected were mapped by using the K/Th map. These zones serve as pathways for the movement of fluids which could react with the granitic rocks. Significant traces of hydrothermally altered zones were mapped at the north-eastern and central to southern part of the study area. The affected regions of alteration also coincide with the regions of major magnetic lineaments observed on the first vertical derivative map and, thus, may represent the regions of potential gold mineralisation. The results obtained in this research agreed with authors such as Kayode (2006), Adelusi *et al.* (2013), Nwokeabia *et al.* (2018) who also proposed that the area is a potential host of commercial gold deposits based on the mapped geological structures, lithology, and hydrothermally altered zones that serve as mineralisation indicators defined from aero-magnetic and aero-radiometric data sets.

This work was carried out in collaboration among all the authors. Author AOK designed the study, wrote the protocol and wrote the first draft of the manuscript. Authors KAS and AUD managed the analyses of the study. Authors LJO, AA and AS performed the statistical analysis and managed the literature searches. All authors read and approved the final manuscript.

REFERENCES

1. A. Aliyu, K. A. Salako, T. Adewumi and A. Mohammed (2018) Interpretation of High Resolution Aeromagnetic Data to Estimate the Curie Point Depth Isotherm of Parts of Middle Benue Trough, North-East, Nigeria Physical Science International Journal 17(3): 1-9,

2. Adelusi A. O., Kayode J. S., and Akinlalu A. A. (2013) Interpretation of aeromagnetic anomalies and electrical resistivity mapping around Iwaraja area Southwestern Nigeria *Journal of Geology and Mining Research* Vol. 5(2) pp. 38-57,

3. Ajeigbe O.M., Adeniran O.J., and Babalola O.A (2014) Mineral Prospecting Potentials Of Osun State. *European Journal of Business and Management*. 6, 115-123.

4. Airo M. L. (2007). Application of Aerogeophysical Data for Gold Exploration: Implications for Central Lapland Greenstone Belt. In: Ojala, J. V. (ed.) Gold in the Central Lapland Greenstone Belt, Finland. Geological Survey of Finland, Special Paper 44; 171–192.

5. Aliyu A., Salako K. A., Adewumi T. and Mohammed A., (*2018)* Interpretation of High-Resolution Aeromagnetic Data to Estimate the Curie Point Depth Isotherm of Parts of Middle Benue Trough, North-East, Nigeria. *Physical Science International Journal 17(3): 1-9.*

6. Boyle, R. (1979). The geochemistry of gold and its deposits (together with a chapter on geochemical prospecting for the element). Geological Survey of Canada.

7. Christopher Akulga, (2013). Investigating Gold Mineralization Potentials in part of the Kibi-Winneba belt of Ghana using Airborne Magnetic and Radiometric Data. Master of Philosophy (Geophysics) Thesis, Kwame Nkrumah University of Science and Technology, Ghana.

8. Dickson B. L. and Scott K. M. (1997). Interpretation of aerial gamma-ray surveys-adding the geochemical factors. *AGSO Journal of Australian Geology and Geophysics*.;17(2):187–200.

9. Fayemi, K. (2017). Mineral Resource Management for National Cohesion and Development. *Paper Delivered at the 5th Annual Lecture of the School of Management Technology, The Federal University of Technology, Akure, Nigeria.*

10. IAEA (International Atomic Energy Agency) 2003 Guidelines for radioelement mapping using gamma ray spectrometry data, Vienna.

11. Junner, N. (1940). The geology of the Gold Coast and western Togoland, 1940. 40 p. *Bull. Geological Survey Gold-Coast, vol. 10*, 40.

12. Kayode, J. S., (2006). Ground Magnetic Study of Jeda-Iloko Area, Southwestern Nigeria and Its Geologic Implications. M. Tech. Thesis, Federal University of Technology, Akure, Nigeria.

13. Keary Philip, Michael Brooks, Ian Hill. (2002). An Introduction to Geophysical Exploration Third Edition. Osney Mead, Oxford OX2 0EL: Blackwell Science Ltd.

14. Mekonnen, T. K. (2004). Interpretation and Geodatabase of Dukes using Aeromagnetic data of Zimbabwe and Mozambique. M. Sc. Thesis, *International Institute for Geoinformation science and Earth Observation, Enschede, the Netherlands*. Retrieved from http://www.slideserve.com/phila/partners.

15. Milligan, P. R. and Gunn, P. J. (1997) Enhancement and Presentation of Airborne Geophysical Data. *Journal of Australian Geology and Geophysics*, vol. 17, pp. 63-75.

16. Mam D. Tawey, Abbass A. Adetona, A., Usman D. Alhassan, Abddulwaheed . A. Rafiu, Kazeem A. Salako and Emmanuel E. Udensi, (2021) Aeroradiometric Data assessment of Hydrothermal alteration Zones in Parts of North Central Nigeria. *Asian Journal of Geological Research* 4(2): 1-16.

17. Nabighian, M.N. (1972): The analytic signal of two-dimensional magnetic bodies with polygonal cross-sections: Its properties and use for automated anomaly interpretation. Geophysics, 37 1972, 507-517.

18. Nicolet J. P. and Erdi-Krausz G. (2003) Guidelines for radioelement mapping using gamma-ray spectrometry data.

19. Nigeria Geological survey Agency (NGSA). Geology map of Nigeria; 2006.

20. Nwokeabia Nkiru, Uche Iduma, Ibe Stephen (2018) Evaluating the Economic Potential of Part of Ife-Ilesha Schist Belt, Western Nigeria, Using Airborne Magnetic and Radiometric Dataset *IOSR Journal of Applied Geology and Geophysics* (IOSR-JAGG) e-ISSN: 2321–0990, p-ISSN: 2321–0982.Volume 6, Issue 4 Ver. I, PP 54-75 www.iosrjournals.org DOI: 10.9790/0990-0604015475

21. Obaje NG. Geology and mineral resources of Nigeria, Berlin: Springer-Verlag, Heidelberg. 2009;221

22. Ogungbemi, Oluwaseun S., Amigun, John O. and Olayanju, Gbenga M., (2018). Geophysical characterization of mineralization p[otential of eastern parts of Ife-Ijesha schist belt, southwestern nigeria. *International Journal of Scientific and tecnology research*. 7(3) ISSN 2277-8616.

23. Ostrovskiy, E. A. (1975). Antagonism of radioactive elements in well rock alteration fields and its use in aero gamma spectrometric prospecting. *International Geological Review*, 17:461–8.

24. Rahaman, M. A. 1976. Review of the Basement Geology of Southwestern Nigeria. In: *Geology of Nigeria*, C. A. Kogbe (Editor). Elizabethan Publication Company, Lagos. 41-58.

25. Reeves C.V (2005) Aeromagnetic Surveys Principles, Practice & Interpretation *Geosoft*

26. Salako (2014). Depth to Basement Determination Using Source Parameter Imaging (SPI) of Aeromagnetic Data: An Application to Upper Benue Trough and Borno Basin, Northeast, Nigeria. Pp 74 -86. *Academic Research International retrieved from* www.journals.savap.org.pk

27. Silva, A. M., Pires, A. C. B., McCafferty, A., Moraes, R. A. V., and Xia, H. (2003). Application of airborne geophysical data to mineral exploration in the uneven exposed terrains of the Rio Das Velhas greenstone belt. Revista Brasileira de Geociências, 33(2):17–28.

28. Slagstad, T. 2008: Radiogenic heat production of Archean to Permian geological provinces in Norway. *Norwegian Journal of Geology* vol. 88, pp 149-166.

29. Tawey, M D,, Alhassan, D. U., Adetona, A. A., Salako, K. A., Rafiu, A. A. and Udensi, E. E., (2020). Application of Aeromagnetic data to assess the Structures and Solid Mineral Potentials in part of North Central Nigeria. *Journal of Geography. Environment and Earth Science International (JGEESI)*, 24(5):11-29.

30. Telford W. M, Geldart L P, Sherriff R. E. and Keys D. A., (1990). Applied geophysics. Cambridge: Cambridge University Press.;860.

31. Thurston J.B., and Smith, R. S., (1997). Automatic conversion of magnetic data to depth, dip, and susceptibility contrast using the Source Parameter Imaging method: *Geophysics*, 62, 807–813, 1997.

32. Wilford J. R., Bierwirth P. N. and Craig M. A. (1997). Application of Airborne Gamma-ray Spectrometry in Soil/Regolith Mapping and Applied Geomorphology. *AGSO Journal of Australian Geology and Geophysics*.;17(2):201-216.